FERMILAB-PUB-15-258-E

Search for Violation of CPT and Lorentz invariance in B_s^0 meson oscillations

V.M. Abazov,[31] B. Abbott,[67] B.S. Acharya,[25] M. Adams,[46] T. Adams,[44] J.P. Agnew,[41] G.D. Alexeev,[31] G. Alkhazov,[35] A. Alton[a],[56] A. Askew,[44] S. Atkins,[54] K. Augsten,[7] C. Avila,[5] F. Badaud,[10] L. Bagby,[45] B. Baldin,[45] D.V. Bandurin,[73] S. Banerjee,[25] E. Barberis,[55] P. Baringer,[53] J.F. Bartlett,[45] U. Bassler,[15] V. Bazterra,[46] A. Bean,[53] M. Begalli,[2] L. Bellantoni,[45] S.B. Beri,[23] G. Bernardi,[14] R. Bernhard,[19] I. Bertram,[39] M. Besançon,[15] R. Beuselinck,[40] P.C. Bhat,[45] S. Bhatia,[58] V. Bhatnagar,[23] G. Blazey,[47] S. Blessing,[44] K. Bloom,[59] A. Boehnlein,[45] D. Boline,[64] E.E. Boos,[33] G. Borissov,[39] M. Borysova[l],[38] A. Brandt,[70] O. Brandt,[20] R. Brock,[57] A. Bross,[45] D. Brown,[14] X.B. Bu,[45] M. Buehler,[45] V. Buescher,[21] V. Bunichev,[33] S. Burdin[b],[39] C.P. Buszello,[37] E. Camacho-Pérez,[28] B.C.K. Casey,[45] H. Castilla-Valdez,[28] S. Caughron,[57] S. Chakrabarti,[64] K.M. Chan,[51] A. Chandra,[72] E. Chapon,[15] G. Chen,[53] S.W. Cho,[27] S. Choi,[27] B. Choudhary,[24] S. Cihangir,[45] D. Claes,[59] J. Clutter,[53] M. Cooke[k],[45] W.E. Cooper,[45] M. Corcoran,[72] F. Couderc,[15] M.-C. Cousinou,[12] J. Cuth,[21] D. Cutts,[69] A. Das,[71] G. Davies,[40] S.J. de Jong,[29,30] E. De La Cruz-Burelo,[28] F. Déliot,[15] R. Demina,[63] D. Denisov,[45] S.P. Denisov,[34] S. Desai,[45] C. Deterre[c],[41] K. DeVaughan,[59] H.T. Diehl,[45] M. Diesburg,[45] P.F. Ding,[41] A. Dominguez,[59] A. Dubey,[24] L.V. Dudko,[33] A. Duperrin,[12] S. Dutt,[23] M. Eads,[47] D. Edmunds,[57] J. Ellison,[43] V.D. Elvira,[45] Y. Enari,[14] H. Evans,[49] A. Evdokimov,[46] V.N. Evdokimov,[34] A. Fauré,[15] L. Feng,[47] T. Ferbel,[63] F. Fiedler,[21] F. Filthaut,[29,30] W. Fisher,[57] H.E. Fisk,[45] M. Fortner,[47] H. Fox,[39] S. Fuess,[45] P.H. Garbincius,[45] A. Garcia-Bellido,[63] J.A. García-González,[28] V. Gavrilov,[32] W. Geng,[12,57] C.E. Gerber,[46] Y. Gershtein,[60] G. Ginther,[45,63] O. Gogota,[38] G. Golovanov,[31] P.D. Grannis,[64] S. Greder,[16] H. Greenlee,[45] G. Grenier,[17] Ph. Gris,[10] J.-F. Grivaz,[13] A. Grohsjean[c],[15] S. Grünendahl,[45] M.W. Grünewald,[26] T. Guillemin,[13] G. Gutierrez,[45] P. Gutierrez,[67] J. Haley,[68] L. Han,[4] K. Harder,[41] A. Harel,[63] J.M. Hauptman,[52] J. Hays,[40] T. Head,[41] T. Hebbeker,[18] D. Hedin,[47] H. Hegab,[68] A.P. Heinson,[43] U. Heintz,[69] C. Hensel,[1] I. Heredia-De La Cruz[d],[28] K. Herner,[45] G. Hesketh[f],[41] M.D. Hildreth,[51] R. Hirosky,[73] T. Hoang,[44] J.D. Hobbs,[64] B. Hoeneisen,[9] J. Hogan,[72] M. Hohlfeld,[21] J.L. Holzbauer,[58] I. Howley,[70] Z. Hubacek,[7,15] V. Hynek,[7] I. Iashvili,[62] Y. Ilchenko,[71] R. Illingworth,[45] A.S. Ito,[45] S. Jabeen[m],[45] M. Jaffré,[13] A. Jayasinghe,[67] M.S. Jeong,[27] R. Jesik,[40] P. Jiang,[4] K. Johns,[42] E. Johnson,[57] M. Johnson,[45] A. Jonckheere,[45] P. Jonsson,[40] J. Joshi,[43] A.W. Jung,[45] A. Juste,[36] E. Kajfasz,[12] D. Karmanov,[33] I. Katsanos,[59] M. Kaur,[23] R. Kehoe,[71] S. Kermiche,[12] N. Khalatyan,[45] A. Khanov,[68] A. Kharchilava,[62] Y.N. Kharzheev,[31] I. Kiselevich,[32] J.M. Kohli,[23] A.V. Kozelov,[34] J. Kraus,[58] A. Kumar,[62] A. Kupco,[8] T. Kurča,[17] V.A. Kuzmin,[33] S. Lammers,[49] P. Lebrun,[17] H.S. Lee,[27] S.W. Lee,[52] W.M. Lee,[45] X. Lei,[42] J. Lellouch,[14] D. Li,[14] H. Li,[73] L. Li,[43] Q.Z. Li,[45] J.K. Lim,[27] D. Lincoln,[45] J. Linnemann,[57] V.V. Lipaev,[34] R. Lipton,[45] H. Liu,[71] Y. Liu,[4] A. Lobodenko,[35] M. Lokajicek,[8] R. Lopes de Sa,[45] R. Luna-Garcia[g],[28] A.L. Lyon,[45] A.K.A. Maciel,[1] R. Madar,[19] R. Magaña-Villalba,[28] S. Malik,[59] V.L. Malyshev,[31] J. Mansour,[20] J. Martínez-Ortega,[28] R. McCarthy,[64] C.L. McGivern,[41] M.M. Meijer,[29,30] A. Melnitchouk,[45] D. Menezes,[47] P.G. Mercadante,[3] M. Merkin,[33] A. Meyer,[18] J. Meyer[i],[20] F. Miconi,[16] N.K. Mondal,[25] M. Mulhearn,[73] E. Nagy,[12] M. Narain,[69] R. Nayyar,[42] H.A. Neal,[56] J.P. Negret,[5] P. Neustroev,[35] H.T. Nguyen,[73] T. Nunnemann,[22] J. Orduna,[72] N. Osman,[12] J. Osta,[51] A. Pal,[70] N. Parashar,[50] V. Parihar,[69] S.K. Park,[27] R. Partridge[e],[69] N. Parua,[49] A. Patwa[j],[65] B. Penning,[40] M. Perfilov,[33] Y. Peters,[41] K. Petridis,[41] G. Petrillo,[63] P. Pétroff,[13] M.-A. Pleier,[65] V.M. Podstavkov,[45] A.V. Popov,[34] M. Prewitt,[72] D. Price,[41] N. Prokopenko,[34] J. Qian,[56] A. Quadt,[20] B. Quinn,[58] P.N. Ratoff,[39] I. Razumov,[34] I. Ripp-Baudot,[16] F. Rizatdinova,[68] M. Rominsky,[45] A. Ross,[39] C. Royon,[15] P. Rubinov,[45] R. Ruchti,[51] G. Sajot,[11] A. Sánchez-Hernández,[28] M.P. Sanders,[22] A.S. Santos[h],[1] G. Savage,[45] M. Savitskyi,[38] L. Sawyer,[54] T. Scanlon,[40] R.D. Schamberger,[64] Y. Scheglov,[35] H. Schellman,[48] M. Schott,[21] C. Schwanenberger,[41] R. Schwienhorst,[57] J. Sekaric,[53] H. Severini,[67] E. Shabalina,[20] V. Shary,[15] S. Shaw,[41] A.A. Shchukin,[34] V. Simak,[7] P. Skubic,[67] P. Slattery,[63] D. Smirnov,[51] G.R. Snow,[59] J. Snow,[66] S. Snyder,[65] S. Söldner-Rembold,[41] L. Sonnenschein,[18] K. Soustruznik,[6] J. Stark,[11] D.A. Stoyanova,[34] M. Strauss,[67] L. Suter,[41] P. Svoisky,[67] M. Titov,[15] V.V. Tokmenin,[31] Y.-T. Tsai,[63] D. Tsybychev,[64] B. Tuchming,[15] C. Tully,[61] L. Uvarov,[35] S. Uvarov,[35] S. Uzunyan,[47] R. Van Kooten,[49] W.M. van Leeuwen,[29] N. Varelas,[46] E.W. Varnes,[42] I.A. Vasilyev,[34] A.Y. Verkheev,[31] L.S. Vertogradov,[31] M. Verzocchi,[45] M. Vesterinen,[41] D. Vilanova,[15] P. Vokac,[7] H.D. Wahl,[44] M.H.L.S. Wang,[45] J. Warchol,[51] G. Watts,[74] M. Wayne,[51] J. Weichert,[21] L. Welty-Rieger,[48] M.R.J. Williams[n],[49] G.W. Wilson,[53] M. Wobisch,[54] D.R. Wood,[55] T.R. Wyatt,[41] Y. Xie,[45]

R. Yamada,[45] S. Yang,[4] T. Yasuda,[45] Y.A. Yatsunenko,[31] W. Ye,[64] Z. Ye,[45] H. Yin,[45] K. Yip,[65] S.W. Youn,[45] J.M. Yu,[56] J. Zennamo,[62] T.G. Zhao,[41] B. Zhou,[56] J. Zhu,[56] M. Zielinski,[63] D. Zieminska,[49] and L. Zivkovic[14]

(The D0 Collaboration)

[1]*LAFEX, Centro Brasileiro de Pesquisas Físicas, Rio de Janeiro, Brazil*
[2]*Universidade do Estado do Rio de Janeiro, Rio de Janeiro, Brazil*
[3]*Universidade Federal do ABC, Santo André, Brazil*
[4]*University of Science and Technology of China, Hefei, People's Republic of China*
[5]*Universidad de los Andes, Bogotá, Colombia*
[6]*Charles University, Faculty of Mathematics and Physics, Center for Particle Physics, Prague, Czech Republic*
[7]*Czech Technical University in Prague, Prague, Czech Republic*
[8]*Institute of Physics, Academy of Sciences of the Czech Republic, Prague, Czech Republic*
[9]*Universidad San Francisco de Quito, Quito, Ecuador*
[10]*LPC, Université Blaise Pascal, CNRS/IN2P3, Clermont, France*
[11]*LPSC, Université Joseph Fourier Grenoble 1, CNRS/IN2P3, Institut National Polytechnique de Grenoble, Grenoble, France*
[12]*CPPM, Aix-Marseille Université, CNRS/IN2P3, Marseille, France*
[13]*LAL, Université Paris-Sud, CNRS/IN2P3, Orsay, France*
[14]*LPNHE, Universités Paris VI and VII, CNRS/IN2P3, Paris, France*
[15]*CEA, Irfu, SPP, Saclay, France*
[16]*IPHC, Université de Strasbourg, CNRS/IN2P3, Strasbourg, France*
[17]*IPNL, Université Lyon 1, CNRS/IN2P3, Villeurbanne, France and Université de Lyon, Lyon, France*
[18]*III. Physikalisches Institut A, RWTH Aachen University, Aachen, Germany*
[19]*Physikalisches Institut, Universität Freiburg, Freiburg, Germany*
[20]*II. Physikalisches Institut, Georg-August-Universität Göttingen, Göttingen, Germany*
[21]*Institut für Physik, Universität Mainz, Mainz, Germany*
[22]*Ludwig-Maximilians-Universität München, München, Germany*
[23]*Panjab University, Chandigarh, India*
[24]*Delhi University, Delhi, India*
[25]*Tata Institute of Fundamental Research, Mumbai, India*
[26]*University College Dublin, Dublin, Ireland*
[27]*Korea Detector Laboratory, Korea University, Seoul, Korea*
[28]*CINVESTAV, Mexico City, Mexico*
[29]*Nikhef, Science Park, Amsterdam, the Netherlands*
[30]*Radboud University Nijmegen, Nijmegen, the Netherlands*
[31]*Joint Institute for Nuclear Research, Dubna, Russia*
[32]*Institute for Theoretical and Experimental Physics, Moscow, Russia*
[33]*Moscow State University, Moscow, Russia*
[34]*Institute for High Energy Physics, Protvino, Russia*
[35]*Petersburg Nuclear Physics Institute, St. Petersburg, Russia*
[36]*Institució Catalana de Recerca i Estudis Avançats (ICREA) and Institut de Física d'Altes Energies (IFAE), Barcelona, Spain*
[37]*Uppsala University, Uppsala, Sweden*
[38]*Taras Shevchenko National University of Kyiv, Kiev, Ukraine*
[39]*Lancaster University, Lancaster LA1 4YB, United Kingdom*
[40]*Imperial College London, London SW7 2AZ, United Kingdom*
[41]*The University of Manchester, Manchester M13 9PL, United Kingdom*
[42]*University of Arizona, Tucson, Arizona 85721, USA*
[43]*University of California Riverside, Riverside, California 92521, USA*
[44]*Florida State University, Tallahassee, Florida 32306, USA*
[45]*Fermi National Accelerator Laboratory, Batavia, Illinois 60510, USA*
[46]*University of Illinois at Chicago, Chicago, Illinois 60607, USA*
[47]*Northern Illinois University, DeKalb, Illinois 60115, USA*
[48]*Northwestern University, Evanston, Illinois 60208, USA*
[49]*Indiana University, Bloomington, Indiana 47405, USA*
[50]*Purdue University Calumet, Hammond, Indiana 46323, USA*
[51]*University of Notre Dame, Notre Dame, Indiana 46556, USA*
[52]*Iowa State University, Ames, Iowa 50011, USA*
[53]*University of Kansas, Lawrence, Kansas 66045, USA*
[54]*Louisiana Tech University, Ruston, Louisiana 71272, USA*
[55]*Northeastern University, Boston, Massachusetts 02115, USA*
[56]*University of Michigan, Ann Arbor, Michigan 48109, USA*
[57]*Michigan State University, East Lansing, Michigan 48824, USA*
[58]*University of Mississippi, University, Mississippi 38677, USA*

[59] University of Nebraska, Lincoln, Nebraska 68588, USA
[60] Rutgers University, Piscataway, New Jersey 08855, USA
[61] Princeton University, Princeton, New Jersey 08544, USA
[62] State University of New York, Buffalo, New York 14260, USA
[63] University of Rochester, Rochester, New York 14627, USA
[64] State University of New York, Stony Brook, New York 11794, USA
[65] Brookhaven National Laboratory, Upton, New York 11973, USA
[66] Langston University, Langston, Oklahoma 73050, USA
[67] University of Oklahoma, Norman, Oklahoma 73019, USA
[68] Oklahoma State University, Stillwater, Oklahoma 74078, USA
[69] Brown University, Providence, Rhode Island 02912, USA
[70] University of Texas, Arlington, Texas 76019, USA
[71] Southern Methodist University, Dallas, Texas 75275, USA
[72] Rice University, Houston, Texas 77005, USA
[73] University of Virginia, Charlottesville, Virginia 22904, USA
[74] University of Washington, Seattle, Washington 98195, USA

(Dated: June 12, 2015)

We present the first search for CPT-violating effects in the mixing of B_s^0 mesons using the full Run II data set with an integrated luminosity of 10.4 fb^{-1} of proton-antiproton collisions collected using the D0 detector at the Fermilab Tevatron Collider. We measure the CPT-violating asymmetry in the decay $B_s^0 \to \mu^\pm D_s^\pm$ as a function of celestial direction and sidereal phase. We find no evidence for CPT-violating effects and place limits on the direction and magnitude of flavor-dependent CPT- and Lorentz-invariance violating coupling coefficients. We find 95% confidence intervals of $\Delta a_\perp < 1.2 \times 10^{-12}$ GeV and $(-0.8 < \Delta a_T - 0.396\Delta a_Z < 3.9) \times 10^{-13}$ GeV.

PACS numbers: 11.30.Cp, 13.20.He, 14.40.Nd

Lorentz invariance requires that the description of a particle is independent of its direction of motion or boost velocity. The Standard Model Extension (SME) [1] provides a framework for potential Lorentz and CPT invariance violation (CPTV), suggesting that such violations can occur at the Planck scale but still result in potentially observable effects at currently available collider energies. The process of neutral meson oscillations is described by a 2×2 effective Hamiltonian with mass eigenvalues of the propagating particles having very small differences between them that drive the oscillation probability. For the B_s^0-$\bar{B}_s^0$ system, the fractional difference between the eigenvalues is of the order of 10^{-12}. Due to this, B_s^0-$\bar{B}_s^0$ oscillations form an interferometric system that is very sensitive to small couplings between the valence quarks and a possible Lorentz-invariance violating field, making it an ideal place to search for new physics [2].

The measurement of the like-sign dimuon asymmetry by the D0 Collaboration [3] shows evidence of anomalously large CP-violating effects. This is currently one of the few significant deviations from the standard model of particle physics. One of the interpretations of this effect could be a CPT-invariant CP violation (CPV) in neutral B-meson mixing. The propagating “light” (L) and “heavy” (H) mass eigenvalues of the B_s^0-$\bar{B}_s^0$ system can be written as [4]:

$$|B_{sL}\rangle \propto p\sqrt{1-\xi_s}|B_s^0\rangle + q\sqrt{1+\xi_s}|\bar{B}_s^0\rangle, \qquad (1)$$

$$|B_{sH}\rangle \propto p\sqrt{1+\xi_s}|B_s^0\rangle - q\sqrt{1-\xi_s}|\bar{B}_s^0\rangle. \qquad (2)$$

If the complex parameter ξ_s is zero, CPT is conserved and CPV is due to $|q/p| \neq 1$ so that the oscillation probability $P(B_s^0 \to \bar{B}_s^0)$ is different from $P(\bar{B}_s^0 \to B_s^0)$. An alternative interpretation is that the asymmetry could arise from T-invariant CPV in B_s^0-$\bar{B}_s^0$ mixing [5] where $|q/p| = 1$, but ξ_s is non-zero so that the probability of non-oscillation or oscillation back to the original state $P(B_s^0 \to B_s^0)$ is different from $P(\bar{B}_s^0 \to \bar{B}_s^0)$. By integrating these two probabilities in time the asymmetry $\mathcal{A}_{\mathrm{CPT}}$ between B_s^0 and $\bar{B}_s^0$ meson decays can be investigated. It can be shown that the CPTV contributions to the 2×2 effective Hamiltonian governing B_s^0-$\bar{B}_s^0$ oscillations depend on the difference between the diagonal mass and decay rate terms [4]:

$$\xi_s = \frac{(M_{11} - M_{22}) - \frac{i}{2}(\Gamma_{11} - \Gamma_{22})}{-\Delta m_s + i\Delta\Gamma_s/2} \approx \frac{-\beta^\mu \Delta a_\mu}{\Delta m_s - i\Delta\Gamma_s/2}, \qquad (3)$$

where Δa_μ is a four vector direction and magnitude in space-time characterizing Lorentz-invariance violation which in the SME is given by $\Delta a_\mu = r_s a_\mu^s - r_b a_\mu^b$ where a_μ^q are Lorentz-violating coupling constants for the two valence quarks in the B_s^0 meson, and where the factors r_q allow for quark-binding or other normalization effects. The four-velocity of the B_s^0 meson is given by $\beta^\mu = \gamma(1, \vec{\beta})$, $\beta^\mu \Delta a_\mu$ is the difference between the diagonal elements of the effective Hamiltonian, and the mass and decay rate differences of the mass eigenstates are $\Delta m_s = m_H - m_L$, and $\Delta\Gamma_s = \Gamma_L - \Gamma_H$ [6]. The small fractional values of Δm_s and $\Delta\Gamma_s$ make the B_s^0 system sensitive to CPTV effects. In the underlying theory, spontaneous Lorentz symmetry breaking generates constant background ex-

pectation values for the quark fields that are Lorentz vectors represented by Δa_μ or tensors instead of scalars [4].

Any observed CPT violation should vary in the frame of the detector denoted with indices (t, x, y, z). The period will be one sidereal day ($\simeq 0.99727$ solar days) as the direction of the proton beam follows the Earth's rotation with respect to the distant stars [4]. In the SME the variation would depend on CPT- and Lorentz-invariance violation coupling coefficients Δa_μ with indices (T, X, Y, Z). We choose (T, X, Y, Z) as coordinates in the standard Sun-centered frame with the rotation axis of the Earth taken as the Z-axis and $X(Y)$ is at right ascension 0° (90°) [7] (see [8] for a diagram of the coordinate system). If CPTV in B_s^0-$\bar{B}_s^0$ oscillations is allowed, then $\mathcal{A}_{\rm CPT} = (\Delta m_s/\Gamma_s)\mathrm{Im}(\xi_s)$ if ξ_s is small. By translating from the Sun-centered frame to the detector frame we have [4]

$$\mathcal{A}_{\rm CPT} = \frac{-\Delta\Gamma_s \gamma^{\rm D0}}{\Gamma_s \Delta m_s} \Big[\Delta a_T - C_\alpha S_\chi \beta_z^{\rm D0} \Delta a_Z + \sqrt{C_\alpha^2 C_\chi^2 + S_\alpha^2}\sin(\Omega\hat{t} + \delta + \kappa)\beta_z^{\rm D0}\Delta a_\perp\Big], \quad (4)$$

where $C_x = \cos(x)$, $S_x = \sin(x)$, $\hat{t}$ is elapsed time with respect to the vernal equinox of the year 2000, $\Omega = 2\pi$ rad/sidereal day, $\beta_z^{\rm D0} = \beta^{\rm D0}\cos\theta$ is the velocity $\vec{\beta}$ of the B_s^0 meson in the detector frame projected onto the z-axis (proton beam direction) of the D0 detector, θ is the polar angle between the B_s^0 momentum and the proton beam direction, $\gamma^{\rm D0} = 1/\sqrt{1-(\beta^{\rm D0})^2}$, χ is the colatitude of the D0 detector, α is the orientation of the z-axis of the detector in the earth's coordinate system, where the proton beam has a bearing of 219.53°, $\Delta a_\perp = \sqrt{\Delta a_X^2 + \Delta a_Y^2}$ is the transverse and Δa_Z the longitudinal components of Δa_μ, $\delta = \tan^{-1}(\Delta a_Y/\Delta a_X)$, $\kappa = \tan^{-1}(-S_\alpha/C_\alpha C_\chi)$ and Δa_T is the time component of the Δa_μ four-vector. A variation with sidereal time could arise from the rotation of $\beta_z^{\rm D0}$ with respect to $\Delta\vec{a}$. In this Letter we place limits on $\Delta a_\perp$ and $\Delta a_T - C_\alpha S_\chi \beta_z^{\rm D0}\Delta a_Z$.

Past experiments and analyses have placed constraints on the flavor-dependent Δa_μ in other neutral meson oscillating systems: K^0-$\bar{K}^0$ [9], D^0-$\bar{D}^0$ [10], and B^0-$\bar{B}^0$ [11], as well as indirect limits for B_s^0-$\bar{B}_s^0$ [5].

This article presents a search for CPT and Lorentz violation using the decay $B_s^0 \to \mu^+ D_s^- X$, where $D_s^- \to \phi\pi^-$ and $\phi \to K^+K^-$ (charge conjugate states are assumed in this article). CP-violating asymmetries are usually between "wrong-sign" decays $B_s^0 \to \bar{B}_s^0 \to \mu^+ D_s^-$, but we want to study the asymmetry between the "right-sign" decays $B_s^0 \to B_s^0 \to \mu^- D_s^+$ and its charge conjugate. We extract the CPT-violating parameter using the asymmetry:

$$A = \frac{N_+ - N_-}{N_+ + N_-}, \quad (5)$$

where N_+ $[N_-]$ is the number of reconstructed $B_s^0 \to \mu^\pm D_s^\mp X$ events where $\mathrm{sgn}(\cos\theta)Q > 0$ $[\mathrm{sgn}(\cos\theta)Q < 0]$ which results from the $\beta_z^{\rm D0} = \beta^{\rm D0}\cos\theta$ terms in Eq. 4 and Q is the charge of the muon. The direction of the $\mu^+ D_s^-$ system differs from that of the parent B_s^0 due to the missing neutrino. However, the migration between N_+ and N_- terms near $\theta = \pi/2$ causes a negligible correction to the measured asymmetry. The initial state at production is not flavor tagged in our study, but after experimental selection requirements, the B_s^0 system is fully mixed, so that the probability of observing a B_s^0 or $\bar{B}_s^0$ is essentially equal regardless of the flavor at production. We assume no CP violation in mixing [12], so only about half of the observed B_s^0 have the same flavor as they had at birth. We assume no CP violation, so those observed B_s^0 mesons which have changed their flavor do not contribute to CPTV, leading to a 50% dilution in the measured asymmetry. In the presence of CPT violation, the asymmetry is expected to have a period of one sidereal day, so a search is made for variations of the form

$$A(\hat{t}) = A_0 - A_1 \sin(\Omega\hat{t} + \phi), \quad (6)$$

where A_0, A_1 and $\phi = \delta + \kappa$ are constants and are extracted by measuring the asymmetry A in Eq. 5 in bins of the sidereal phase $\Omega\hat{t}$, and fitting to the value in each bin with Eq. 6. Measurements of A_0 and A_1 are then interpreted as limits on Δa_μ from B_s^0-$\bar{B}_s^0$ oscillations. A non-zero value of Δa_z and Δa_T would lead to a CPTV asymmetry that does not vary with sidereal time.

The data selection and the signal extraction are identical to those used in Ref. [13]. The main details of the data selection using the D0 detector [14] are described here.

The data are collected with a suite of single and dimuon triggers. The selection and reconstruction of $\mu^+ D_s^- X$ decays require tracks with at least two hits in both the central fiber tracker and the silicon microstrip tracker. The muon track segment outside the calorimeter has to be matched to a particle found in the central tracking system which has momentum $p > 3$ GeV and transverse momentum $2 < p_T < 25$ GeV. The $D_s^- \to \phi\pi^-$, $\phi \to K^+K^-$ decay is reconstructed by assuming the two ϕ decay particles are kaons, requiring $p_T > 0.7$ GeV, opposite charges, and $M(K^+K^-) < 1.07$ GeV. The charge of the third particle, assumed to be the charged pion, must have charge opposite to that of the muon and $0.5 < p_T < 25$ GeV. The three tracks are combined to create a common D_s^- decay vertex using the algorithm described in Ref. [15]. The reconstructed $\mu^\pm D_s^\mp$ candidate is required to pass several kinematic selection criteria and satisfy likelihood ratio criteria that are identical to those described in Ref. [13].

The effective $K^+K^-\pi^\pm$ mass distribution is fitted using bins of 6 MeV over a range of $1.7 < M(K^+K^-\pi^\pm) < 2.3$ GeV, and the number of signal and background events is extracted by a χ^2 fit of an empirical model to the data. The $D_s^\pm$ meson mass distribution is well modeled by two

Gaussian functions constrained to have the same mean, but with different widths and normalizations. There is negligible peaking background under the $D_s^{\pm}$ peak. A second peak in the $M(K^+K^-\pi^{\pm})$ distribution corresponding to the Cabibbo-suppressed $D^{\pm} \to \phi\pi^{\pm}$ decay is also modeled by two Gaussian functions with widths set to those of the $D_s^{\pm}$ meson model scaled by the ratio of the fitted $D^{\pm}$ and $D_s^{\pm}$ masses. The combinatoric background is modeled by a 5$^{\mathrm{th}}$-order polynomial function. Partially reconstructed decays such as $D_s^{\pm} \to \phi\pi^{\pm}\pi^0$ where the π^0 is not reconstructed are modeled with a threshold function that extends to the $D_s^{\pm}$ mass after the π^0 mass has been subtracted, given by $T(m) = \tan^{-1}\left[p_1(mc^2 - p_2)\right] + p_3$, where p_i are fit parameters.

The raw asymmetry (Eq. 5) is extracted by fitting the $M(K^+K^-\pi^{\pm})$ distribution of the $\mu^{\pm}D_s^{\mp}$ candidates using a χ^2 minimization. The fit is performed simultaneously, using the same models, on the sum and the difference of the $M(K^+K^-\pi^{\pm})$ distribution of N_+ candidates and N_- candidates. The functions used to model the two distributions are

$$W_{\mathrm{sum}} = W_{D_s} + W_D + W_{\mathrm{cb}} + W_{\mathrm{pt}}, \tag{7}$$

$$W_{\mathrm{diff}} = AW_{D_s} + A_D W_D + A_{\mathrm{cb}}W_{\mathrm{cb}} + A_{\mathrm{pt}}W_{\mathrm{pt}}, \tag{8}$$

where W_{D_s}, W_D, W_{cb}, and W_{pt} describe the distribution of the $D_s^{\pm}$ and $D^{\pm}$ mass peaks, the combinatorial background, and the partially reconstructed events, respectively, and the A factors are the corresponding asymmetries which are extracted from the fit. The number of signal events in the sample is $N(D_s^{\pm}) = 205{,}865 \pm 626$.

Following previous conventions [16] we shift the origin of the time coordinate to correspond to the vernal equinox of the year 2000. The value of A_1 is extracted by dividing the data into n data sets, each containing a fraction f_i of the data based on the sidereal phase $\Omega\hat{t}+\phi$. In the fit, the parameters that describe the mass distributions W_{sum} and W_{diff} are the same for all sidereal bins, except for A and A_D which may vary with sidereal phase.

The number of sidereal bins used to extract the asymmetry is determined by finding the smallest uncertainty on A_1. By using MC input of asymmetries from 0% to 2% we find that the optimum number of bins is eleven. One of the eleven distributions produced in the fit to the data is shown in Fig. 1.

Systematic uncertainties of the fitting method on the extracted values of A in sidereal bin i, $A(i)$, are evaluated by varying the fitting procedure and are assigned to be half of the maximal variation in the asymmetry. The mass range of the fit is shifted from $1.700 < M(K^+K^-\pi^{\pm}) < 2.300$ GeV to $1.724 < M(K^+K^-\pi^{\pm}) < 2.270$ GeV in steps of 6 MeV resulting in an absolute uncertainty on the measured asymmetries of 0.035%. The width of the mass bins is changed between 1 and 12 MeV resulting in an absolute uncertainty of 0.071%. The functions modelling the signal are modified to fit the $D^{\pm}$ and $D_s^{\pm}$ mass peaks by single Gaussian functions, the background is fitted by varying between a fourth- and seventh-order polynomial function, and the parameter p_1 in the threshold function is allowed to vary. As a test, the fraction of data in each sidereal bin, f_i is fixed to exactly 1/11. These variations of the signal modelling yield an absolute uncertainty on the asymmetry of 0.085%. The uncertainty for each of these sources is added in quadrature, to give the total systematic uncertainty of the fitting procedure of 0.12%. This uncertainty on the measured values of $A(i)$ is found to be independent of sidereal bin, and is added in quadrature to the statistical uncertainty to extract the CPT-violating parameters by fitting to Eq. 6 (see Table I). The measured values of the asymmetries, $A(i)$, are plotted in Fig. 2 and are tabulated in [8].

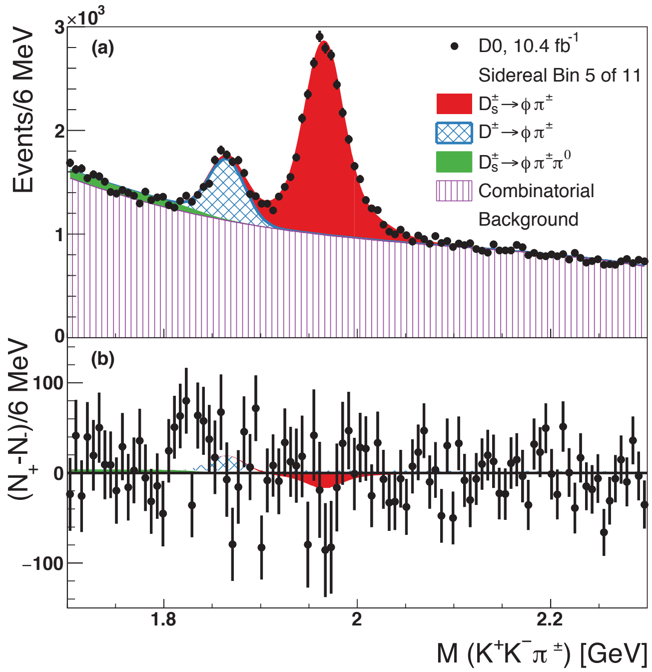

FIG. 1. (a) The $K^+K^-\pi^{\mp}$ invariant mass distribution for one of the 11 sidereal bins of the data (bin 5) of the $\mu^{\pm}\phi\pi^{\mp}$ sample. The lower mass peak is due to the decay $D^{\mp} \to \phi\pi^{\mp}$ and the second peak is due to the $D_s^{\mp}$ meson decay. (b) The fit to the $(N_+ - N_-)$ distribution for one of the 11 sidereal bins of the data (bin 5).

The limits on Δa_{μ} are extracted using:

$$A_1 \sin(\Omega\hat{t}+\phi) = \frac{F^{\text{non-osc}}_{B_s^0}\Delta\Gamma_s\langle\gamma^{D^0}\beta_z^{D^0}\rangle}{\Gamma_s\Delta m_s} \times \sqrt{C_\alpha^2 C_\chi^2 + S_\alpha^2}\sin(\Omega\hat{t}+\delta+\kappa)\Delta a_{\perp}, \tag{9}$$

$$A_0 = -\frac{F^{\text{non-osc}}_{B_s^0}\Delta\Gamma_s\langle\gamma^{D^0}\rangle}{\Gamma_s\Delta m_s}\left[\Delta a_T - C_\alpha S_\chi\langle\beta_z^{D^0}\rangle\Delta a_Z\right], \tag{10}$$

where angle brackets denote average values. The $F^{\text{non-osc}}_{B_s^0}$

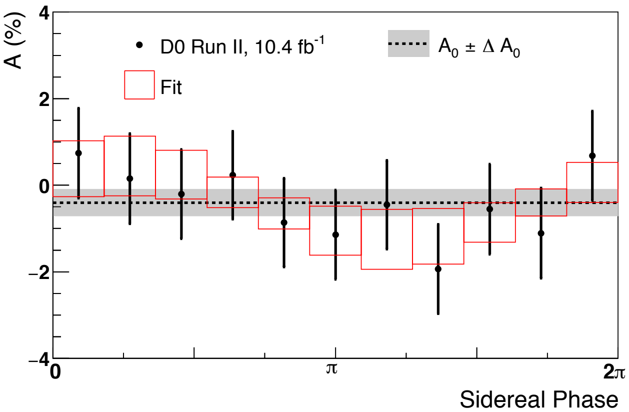

FIG. 2. The measured asymmetries, $A(i)$ versus sidereal phase. The uncertainty on each value of $A(i)$ is the sum in quadrature of the statistical and systematic uncertainties. The red boxes show the fit and its uncertainties to the data points (Eq. 6). The dashed line shows the extracted value of A_0 and the grey box shows ΔA_0.

factor is the fraction of $D_s^\pm \to \phi\pi^\pm$ decays for which an observed B_s^0 has the same flavor as at birth [13]. Combining the fraction of B_s^0 decays in the sample and the 50% dilution factor described earlier gives $F_{B_s^0}^{\text{non-osc}} = 0.465$. Limits are extracted from the probability distribution which is given by $\exp(-\chi^2/2)$ where χ^2 is the chi-square as a function of A_1, A_0 and δ using Eq. 6. Since we are setting limits, the probability distribution will be characterized by two quantities, the most probable value of A_1 and the 95% upper limit (UL) which is extracted by integrating the normalized probability distribution at the value of δ that gives the most conservative limit.

To extract limits, we measure the average values of $\langle\gamma^{\text{D0}}\rangle = \langle E_{B_s^0}\rangle/m_{B_s^0}$, $\langle\beta_z^{\text{D0}}\rangle = \langle p_z\rangle/\langle E_{B_s^0}\rangle$ and $\langle\gamma^{\text{D0}}\beta_z^{\text{D0}}\rangle = \langle p_z\rangle/m_{B_s^0}$ where $\langle p_z\rangle$ is the average momentum in the z-direction and $\langle E_{B_s^0}\rangle$ is the average energy of the B_s^0 meson. The average momentum of the $\mu D_s^\pm$ candidates is measured using sideband subtraction. The signal region is $1.92 < M(K^+K^-\pi^-) < 2.00$ GeV and the sideband regions are $1.75 < M(K^+K^-\pi^-) < 1.79$ GeV and $2.13 < M(K^+K^-\pi^-) < 2.17$ GeV, and the average is $\langle p\rangle = 21.41 \pm 0.03$ GeV. This momentum needs to be corrected for the missing neutrino in the decay using a k-factor correction. These k-factors are taken from Ref. [17] and applied to give a momentum of $\langle p\rangle = 25.3$ GeV. The systematic uncertainty on $\langle p\rangle$ of 1.6 GeV is obtained from the difference between the momentum extracted using sideband subtraction and using a weighted average of the number of signal events in momentum bins which is then added in quadrature to the uncertainty due to the k-factors. The effect of possible reconstruction variations in the x and y directions are found to be less than 1%. If we vary the number of sidereal bins the most probable value of A_1 varies by 8%. These variations are added in quadrature as the relative systematic uncertainty on the value of A_1.

The final results are obtained by scaling the probability distributions obtained for A_0, A_1 with the multiplicative factors given in Table I. The systematic uncertainties on the multiplicative factors, the number of sidereal bins, and reconstruction effects are included by convoluting the probability distribution with a Gaussian function with the width given by the sum in quadrature of the systematic uncertainties. We obtain a 95% upper limit (UL) of $\Delta a_\perp < 1.2 \times 10^{-12}$ GeV. The most probable values of δ and $\Delta a_\perp$ are $\delta = 4.901$ and $\Delta a_\perp = 5.7 \times 10^{-13}$ GeV.

TABLE I. Parameters and uncertainties in the extraction of the CPT-violating parameters. The uncertainties on A_0, A_1 and ϕ are fit uncertainties and are dominated by the statistical uncertainty of the raw asymmetries. All other uncertainties are systematic.

Parameter	Value	Ref.
A_0	$(-0.40 \pm 0.31)\%$	Eq. 6
A_1	$(0.87 \pm 0.45)\%$	Eq. 6
ϕ	-2.28 ± 0.51	Eq. 6
$m_{B_s^0}$	(5.36677 ± 0.00024) GeV	[18]
Δm_s	$(17.761 \pm 0.022) \times 10^{12}\ \hbar\text{s}^{-1}$	[18]
$\Delta\Gamma_s/\Gamma_s$	(0.138 ± 0.012)	[18]
$F_{B_s^0}^{\text{non-osc}} = F_{B_s^0}^{\text{osc}}$	(0.465 ± 0.017)	[13]
$\langle p_z\rangle$	(17.8 ± 1.6) GeV	
$\langle p\rangle$	(25.3 ± 2.3) GeV	
Proton beam dir$^{\text{n}}$ α	$219.53°$	
Colatitude χ	$48.17°$	

The limit on $\Delta a_T - C_\alpha S_\chi \beta_z^{\text{D0}} \Delta a_Z$ is obtained from a fit to the asymmetries using Eq. 6. This results in a value of $A_0 = (-0.40 \pm 0.31)\%$. In this case the systematic uncertainties on the measured values of $A(i)$ are assumed to be 100% correlated between sidereal bins to obtain the most conservative limits and are added to the statistical uncertainty obtained from the fit. Using Eq. 10, we obtain $\Delta a_T - C_\alpha S_\chi \beta_z^{\text{D0}} \Delta a_Z = \Delta a_T - 0.396\Delta a_Z = (1.5 \pm 1.2) \times 10^{-13}$ GeV resulting in a two sided 95% confidence interval $(-0.8 < \Delta a_T - 0.396\Delta a_Z < 3.9) \times 10^{-13}$ GeV.

We did a cross check using the periodogram methodology [19] which sees no anomalous behavior for the frequency 1/sidereal day [8].

For CPTV to explain the difference between the like-sign dimuon asymmetry [3] and the SM requires that $(\Delta a_T - 0.396\Delta a_Z)$ to be of the order of 10^{-12} GeV [5]. These limits imply that CPT violation is unlikely to contribute a significant fraction of the observed dimuon charge asymmetry, and that other explanations need to be sought.

In conclusion, we have carried out the first search for CPT-violating effects exclusively in the B_s^0-$\bar{B}_s^0$ oscillation system via semileptonic decays of the B_s^0 mesons. We find no significant evidence for CPT-violating effects

and place limits on the size of the Lorentz violating effects, Δa_μ. These limits constrain a linear combination of the Lorentz-violating coupling constants a^q_μ for the b and s valence quarks in the B^0_s meson that are different from the linear combinations of valence quarks in the B^0 [11] or K^0 [9] mesons, and therefore further constrain the possible separate values of the three coefficients a^b_μ, a^s_μ, and a^d_μ. We find 95% confidence intervals for the flavor-dependent coefficients $\Delta a_\perp < 1.2 \times 10^{-12}$ GeV and $(-0.8 < \Delta a_T - 0.396 \Delta a_Z < 3.9) \times 10^{-13}$ GeV.

We thank A. Kostelecký for valuable conversations during the course of this work. We also thank the staffs at Fermilab and collaborating institutions, and acknowledge support from the Department of Energy and National Science Foundation (United States of America); Alternative Energies and Atomic Energy Commission and National Center for Scientific Research/National Institute of Nuclear and Particle Physics (France); Ministry of Education and Science of the Russian Federation, National Research Center "Kurchatov Institute" of the Russian Federation, and Russian Foundation for Basic Research (Russia); National Council for the Development of Science and Technology and Carlos Chagas Filho Foundation for the Support of Research in the State of Rio de Janeiro (Brazil); Department of Atomic Energy and Department of Science and Technology (India); Administrative Department of Science, Technology and Innovation (Colombia); National Council of Science and Technology (Mexico); National Research Foundation of Korea (Korea); Foundation for Fundamental Research on Matter (The Netherlands); Science and Technology Facilities Council and The Royal Society (United Kingdom); Ministry of Education, Youth and Sports (Czech Republic); Bundesministerium für Bildung und Forschung (Federal Ministry of Education and Research) and Deutsche Forschungsgemeinschaft (German Research Foundation) (Germany); Science Foundation Ireland (Ireland); Swedish Research Council (Sweden); China Academy of Sciences and National Natural Science Foundation of China (China); and Ministry of Education and Science of Ukraine (Ukraine). We also acknowledge support from the Indiana University Center for Spacetime Symmetries (IUCSS).

[1] V.A. Kostelecký and S. Samuel, *Spontaneous breaking of Lorentz symmetry in string theory*, Phys. Rev. D **39**, 683 (1989); V.A. Kostelecký and R. Potting, *CPT and strings*, Nucl. Phys. B **359**, 545 (1991).

[2] V.A. Kostelecký and R. Potting, *CPT, strings, and meson factories*, Phys. Rev. D **51**, 3923 (1995).

[3] V. M. Abazov *et al.* (D0 Collaboration), *Study of CP-violating charge asymmetries of single muons and like-sign dimuons in $p\bar{p}$ collisions*, Phys. Rev. D **89**, 012002 (2014).

[4] V.A. Kostelecký, *CPT, T, and Lorentz violation in neutral-meson oscillations*, Phys. Rev. D **64**, 076001 (2001); V.A. Kostelecký, *Sensitivity of CPT Tests with Neutral Mesons*, Phys. Rev. Lett. **80**, 1818 (1998); V.A. Kostelecký and R. Van Kooten, *Bounding CPT violation in the neutral B system*, Phys. Rev. D **54**, 5585 (1996).

[5] V.A. Kostelecký and R. Van Kooten, *CPT violation and B-meson oscillations*, Phys. Rev. D **82**, 101702(R) (2010).

[6] This is the convention of the definition of $\Delta\Gamma_s$ so that it is positive in the standard model.

[7] V.A. Kostelecký and C. D. Lane, *Constraints on Lorentz violation from clock comparison experiments*, Phys. Rev. D **60**, 116010 (1999); V.A. Kostelecký and N. Russell, *Data Tables for Lorentz and CPT Violation*, Rev. Mod. Phys. **83**, 11 (2011).

[8] See Supplemental Material at http://link.aps.org/supplemental/10.1103/PhysRevLett.115.161601 for additional plots supporting the analysis, including diagrams of the coordinate system, the measured values of A, and a brief description of the periodogram analysis.

[9] D. Babusci *et al.* (KLOE Collaboration), *Test of CPT and Lorentz symmetry in entangled neutral kaons with the KLOE experiment*, Phys. Lett. B **730**, 89 (2014).

[10] J.M. Link *et al.* (FOCUS Collaboration), *Charm system tests of CPT and Lorentz invariance with FOCUS*, Phys. Lett. B **556**, 7 (2003).

[11] B. Aubert *et al.* (BaBar Collaboration), *Search for CPT and Lorentz violation in B^0-$\bar{B}^0$ oscillations with dilepton events*, Phys. Rev. Lett. **100**, 131802 (2008); K. Abe *et al.* (Belle Collaboration), *Measurement of B^0_d- $\bar{B}^0_d$ mixing rate from the time evolution of dilepton events at the Υ_{4S}*, Phys. Rev. Lett. **86**, 3228 (2001); K. Ackerstaff *et al.* (OPAL Collaboration), *A Study of B meson oscillations using hadronic Z^0 decays containing leptons*, Z. Phys. C **76**, 401 (1997).

[12] Y. Amhis et al., *Averages of b-hadron, c-hadron, and τ-lepton properties as of summer 2014*, arXiv:1412.7515 and online update at http://www.slac.stanford.edu/xorg/hfag

[13] V. M. Abazov *et al.* (D0 Collaboration), *Measurement of the Semileptonic Charge Asymmetry using $B^0_s \to \mu^+ D^-_s X$ Decays* Phys. Rev. Lett. **110**, 011801 (2013).

[14] V. M. Abazov *et al.* (D0 Collaboration), *The upgraded D0 detector*, Nucl. Instrum. Methods Phys. Res. A **565**, 463 (2006).

[15] J. Abdallah *et al.* (DELPHI Collaboration), *b-tagging in DELPHI at LEP*, Eur. Phys. J. C **32**, 185 (2004).

[16] V.A. Kostelecký and N. Russell, *Data tables for Lorentz and CPT violation*, Rev. Mod. Phys. **83**, 11 (2011).

[17] V. M. Abazov *et al.* (D0 Collaboration), *Measurement of the B^0_s Lifetime in the Flavor-Specific Decay Channel $B^0_s \to \mu^+ D^-_s \nu X$*, Phys. Rev. Lett. **114**, 062001 (2015).

[18] K.A. Olive *et al.* (Particle Data Group), *Review of Particle Physics*, Chin. Phys. C, 38, 090001 (2014).

[19] J. D. Scargle, *Studies in astronomical time series analysis. II - Statistical aspects of spectral analysis of unevenly spaced data*, Astrophys. J. 263, 835 (1982), N. R. Lomb, *Least-squares frequency analysis of unequally spaced data*, Astrophys. Space Sci. 39, 447 (1976).

AUXILIARY MATERIAL

To appear as an Electronic Physics Auxiliary Publication (EPAPS)

COORDINATE SYSTEM

We choose (T, X, Y, Z) as coordinates in the standard Sun-centered frame with T being the time coordinate, the rotation axis of the Earth taken as the choice for the Z-axis and $X(Y)$ is at right ascension 0° (90°) (c.f. Ref. [7] of the paper). This coordinate system is illustrated in Fig. 3.

MEASURED ASYMMETRIES

The measured asymmetries, $A(i)$, used to extract the limits are given in Table II.

TABLE II. The measured asymmetries, $A(i)$ versus sidereal phase. The uncertainty on each value of $A(i)$ is the sum in quadrature of the statistical and systematic uncertainties.

Asymmetry	Sidereal Phase	Value (%)
$A(1)$	$0 \to (2\pi)/11$	$+0.74 \pm 1.03$
$A(2)$	$(2\pi)/11 \to 2(2\pi)/11$	$+0.15 \pm 1.03$
$A(3)$	$2(2\pi)/11 \to 3(2\pi)/11$	-0.20 ± 1.02
$A(4)$	$3(2\pi)/11 \to 4(2\pi)/11$	$+0.23 \pm 1.01$
$A(5)$	$4(2\pi)/11 \to 5(2\pi)/11$	-0.86 ± 1.02
$A(6)$	$5(2\pi)/11 \to 6(2\pi)/11$	-1.14 ± 1.02
$A(7)$	$6(2\pi)/11 \to 7(2\pi)/11$	-0.45 ± 1.02
$A(8)$	$7(2\pi)/11 \to 8(2\pi)/11$	-1.93 ± 1.03
$A(9)$	$8(2\pi)/11 \to 9(2\pi)/11$	-0.55 ± 1.03
$A(10)$	$9(2\pi)/11 \to 10(2\pi)/11$	-1.11 ± 1.03
$A(11)$	$10(2\pi)/11 \to (2\pi)$	$+0.68 \pm 1.03$

PERIODOGRAM ANALYSIS

As a cross check to fitting the data for a periodic signal, we also use the periodogram [18] method to measure the spectral power of a signal over a large range of frequencies. The spectral power at a test frequency ν is

$$P(\nu) \equiv \frac{\left| \sum_{j=1}^{N} w_j \exp\left(-2\pi i \nu \hat{t}_j\right) \right|^2}{N \sigma_w^2}, \tag{11}$$

where the data has N measurements each of weight w_j where the weight is the probability that the event is a signal event with a variance σ_w. The weight for each event depends on $Q_j \cos\theta_j$, and $M(K^+K^-\pi^\pm)$ for the event and is based on the fit to Eq. 7: $w_j = Q_j \cos\theta_j W_{D_s}[M(K^+K^-\pi^\pm)]/W_{\rm sum}[M(K^+K^-\pi^\pm)]$. In the absence of an oscillatory signal, the probability that $P(\nu)$ at frequency ν would exceed an observed value S is $P(\nu) > S = \exp(-S)$.

The spectral power of this data sample is $P(\text{one sidereal day}) = 0.65$. The probability of obtaining a value of P greater than this is 52% which is consistent with no signal. The spectral power values for periods from 0.5 to 1.5 solar days in steps of 1 solar day/1000 are shown in Fig. 4. Sixty percent of these measurements are greater than the spectral power at one sidereal day. The 95% UL is obtained by injecting simulated signals into the data and determining the probability distribution of the spectral power as a function of the injected signal A_1. The resulting 95% UL on A_1 is 1.03%. This converts to a 95% UL of $\Delta a_\perp < 6.9 \times 10^{-13}$ GeV which is comparable to that obtained from the analysis of the amplitudes.

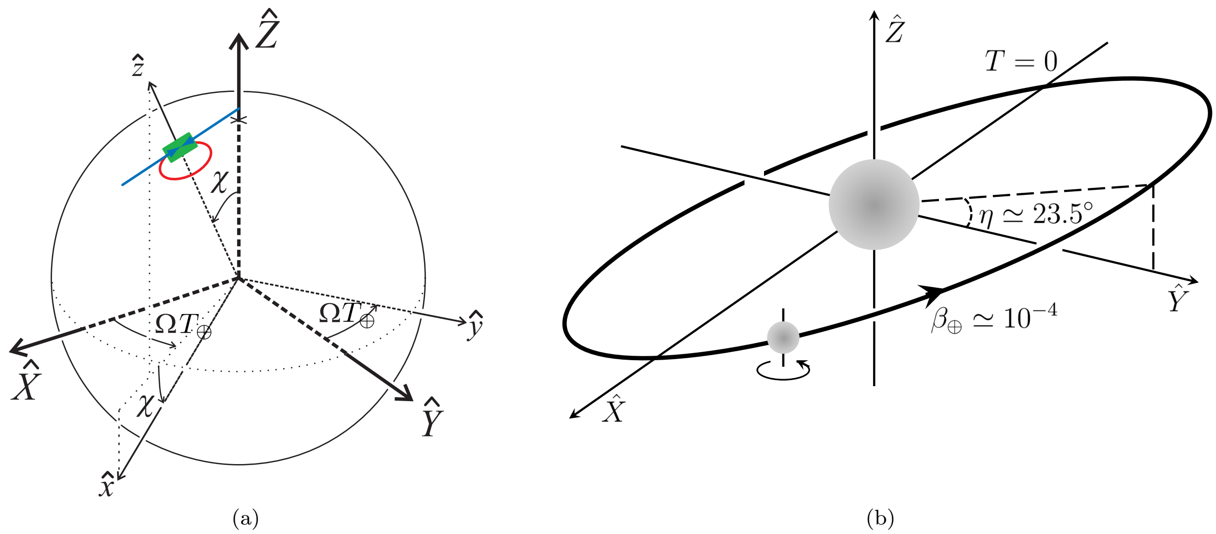

FIG. 3. Illustrations of the coordinate systems used in this analysis. (a) The small rectangle represents the position of the D0 detector on the earth. (b) Orbit of Earth in Sun-based frame (based on Fig. 1 from Ref. [7]).

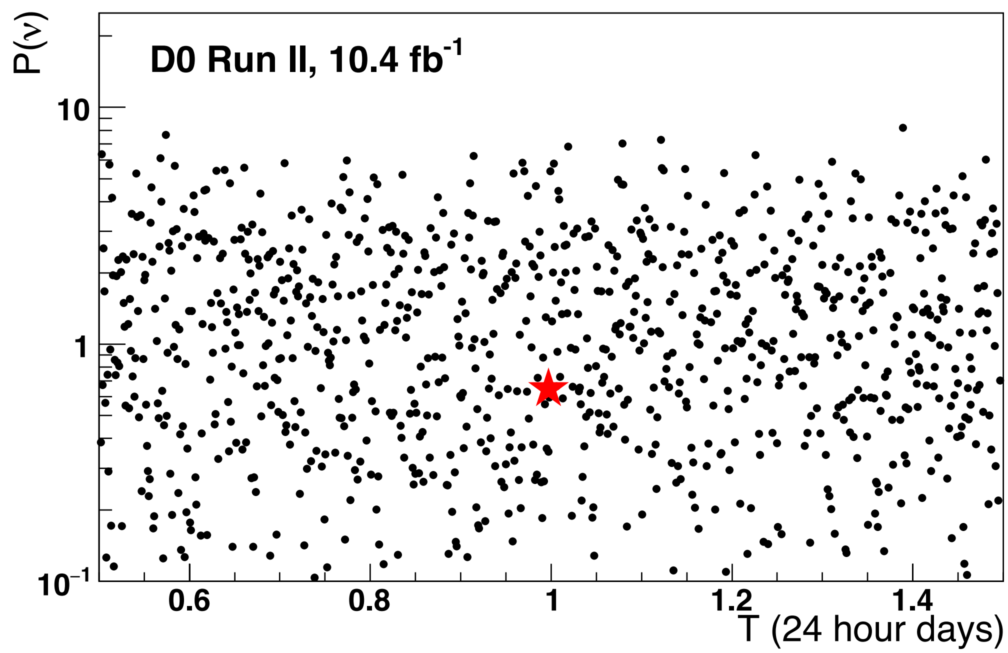

FIG. 4. The periodogram for the B_s^0 data sample over the range of 0.5 days to 1.5 days in steps of (1 day/1000). The red star indicates the spectral power calculated at one sidereal day.